Journal of Physics:
Conference Series

PAPER • **OPEN ACCESS**

Design and development of an autonomous unmanned aerial vehicle for surface coalmines surveillance

To cite this article: Aayush Kumar *et al* 2023 *J. Phys.: Conf. Ser.* **2601** 012003

Design and development of an autonomous unmanned aerial vehicle for surface coalmines surveillance

[1]Aayush Kumar, [2]Abhigyan, [3]Ansh Khanduri, [4]P K Jain

Department of Mechanical Engineering, Delhi Technological University, Main Bawana Road, New Delhi – 110042, India

Corresponding Author: - Abhigyan (nandanrockers@gmail.com)

Abstract. This paper presents a detailed investigation into the development of a specialized unmanned aerial vehicle (UAV) for practical applications in coal mining. The main focus is on enhancing surveillance capabilities, identifying potential hazards, and supporting various coal mine activities. This study initiates with the careful design of a quadcopter, taking into account essential parameters such as VTOL, maneuverability, and hover efficiency. The quadcopter model is meticulously developed to ensure smooth operation under ideal conditions. The design process involves utilizing SolidWorks software to create a robust and optimized quadcopter model. Additionally, the static deformation simulation of the quadcopter is conducted using Ansys software, providing valuable insights into its structural integrity and performance. Dynamic modelling using the Bond Graph Method enables a thorough understanding of the quadcopter's behavior and informs propulsion system selection. The chosen propulsion system prioritizes maximizing thrust-to-weight ratio to about 2:1, achieving the factor of safety of approximately 4, and ensuring maneuverability. The use of eCalc, an online open-source software, assists in identifying the ideal motor-propeller combination for optimal thrust characteristics. Surveillance and mapping techniques are explored in detail. A step-by-step methodology is proposed for image identification, while mapping is achieved through image stitching and path planning using waypoints. Additionally, volume estimation and vulnerability assessment methods specific to coal mining are discussed.

1. Introduction

The mining industry has always been a challenging field, and in recent years, the need for efficient and safe mining operations has become even more critical. The use of unmanned aerial vehicles (UAVs), also known as drones, has become increasingly popular in the mining industry as a tool for monitoring and surveying large areas of land. In particular, the use of UAVs for surface coalmine surveillance [1] has gained significant attention as it offers many benefits such as real-time monitoring, hazard detection, and vulnerability evaluation.

The development of an autonomous UAV for surface coal mine surveillance is a complex task that involves integrating various technologies, such as computer vision, artificial intelligence, and sensor systems[2]. The UAV will be equipped with advanced sensors, including cameras, lidar[3], and thermal imaging, that can collect data from the surface coal mine environment. This data will then be analyzed by computer vision and artificial intelligence algorithms to detect potential hazards and evaluate vulnerabilities.

The UAV will also be equipped with advanced hazard detection and vulnerability evaluation capabilities. For example, the UAV can detect potential hazards such as gas leaks, rock falls, and landslides, and evaluate the vulnerability of the mine infrastructure to these hazards. This information can then be used to take timely and effective interventions to improve the safety and efficiency of mining operations[4].

The UAV will also be able to provide detailed and accurate mapping of the surface coal mine environment, which can be used for a variety of purposes, including mine planning, resource management, and environmental monitoring. For example, the UAV can produce detailed 3D models of the mine, which can be used to plan mining operations and identify areas of the mine that are most suitable for mining. Using UAVs for surface coal mine surveillance is the ability to monitor and survey large areas of land in real-time. This can greatly benefit the mining industry by providing valuable insights into the condition of the mine and identifying potential risks before they become major issues. The autonomous nature of the UAV will increase the coverage area, reduce human intervention, and enhance the overall performance of the system.

2. UAV Design

Conceptual Design parameters We are using a Quadcopter Design in the first stage of our project. A quadcopter is good for surveillance of mines due to its lightweight, compactness, hover efficiency, VTOL, and simplicity of structure.

Table 1. Trade Off Study Between Various Systems.

Weightage	Selection Criteria	Single Rotor	Multi Rotor	Fixed Wing	Fixed Wing Hybrid
10	Compactness	10	8	5	6
10	Reliability	5	7	9	9
10	Simplicity of Structure	8	7	7	6
9	Payload Packaging	4	6	8	8
8	Controllability	4	6	8	8
8	Maturity of Technology	10	8	9	8
8	Hover Efficiency	8	10	0	10
8	VTOL	9	10	0	10
8	Simplicity of Control Systems	8	7	9	7
7	Cruise Efficiency	7	6	9	9
6	Aerodynamic Cleanliness	8	7	8	7
3	Aerodynamic Interaction	7	8	8	9
3	Manoeuvrability	5	7	8	7
	TOTAL	**711**	**731**	**658**	**788**

2.1. Factors considered while designing Quadcopter

1. Endurance
2. Load Carrying Capacity
3. Range/Flight Time
4. Gross Weight
5. Required Payload Capacity

We have chosen multi-rotor quadcopter by considering above factors

2.2. Quadcopter Subcomponents

1. CF X Shaped Frame
2. DC Brushless Motors
3. GPS/GNSS modules with Mount
4. Stereo Camera,2.5D Camera with Mounts/Sensors (EO/IR, Thermal Imaging, Lidar, Sonar)
5. Battery, Flight Controller with Mounts
6. IMU COVER, CF Stand for support with Anti-Skid Rubber Gripper.
7. Propellers, Pixhawk, barometer, PMU (Power management system)

Table 2. Weight estimation of subcomponents.

UAV Component Name	Description	Estimated Range of Weight of each Component (grams)
UAV Frame	X Frame	600-800
Motors and Propeller	4 sets. Approx thrust required = 1.5 times weight	1000 to 1400
Batter	24V, 20-30 min flight time	3500 to 4200
Flight Controller	Pixhawk Cube Orange	150
On-Board Computer	Jetson	300
Other on-board electronics	Powering system and connector cables	100
Payload	Cameras and sensors (swappable)	1000 to 2000

3. Dynamic Modelling

The bond graph method-based dynamic model of the quadcopter is presented in the following paragraphs. Six degrees of freedom (DOF) and four propellers on the quadcopter being discussed in this literature enable translational and rotational motion. The bond graph modelling created by Bhandari et al [5] in their paper, in which they considered a comparable H-shaped quadcopter for their study, is the foundation for the dynamic modelling that follows. The H-drone's i-th propeller's generated thrust force (Fi) and moment (Mi) are given by –

$$F_i = k_f \omega^2 \quad (1)$$

$$M_i = k\ \omega^2 \quad (2)$$

here, coefficients of thrust and drag are represented by kf and km respectively and ωi represents the angular velocity of each propeller [6].

The bond graph of the propeller is depicted in the figure below. The propeller motor's voltage, Vi, is a controlled effort. The motor's armature coil inductance is denoted by Lc, and its resistance by Rc. The motor constant, μ, is a conversion factor that translates the electrical current

provided to the propeller into torque. The rotor inertia of the propeller is represented by J, while the damping resistance is represented by R. The Fi and Mi values are computed from the propeller bond graph based on equations (1)-(2).

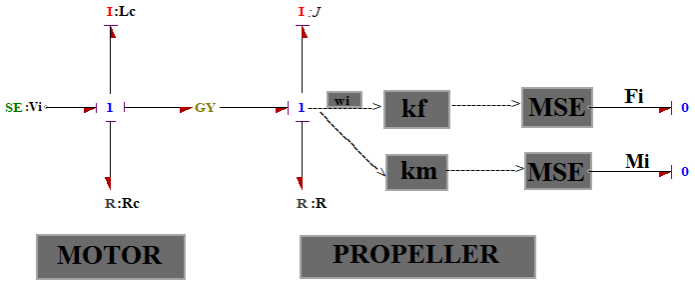

Figure 1. Bond Graph of the Propeller using (Symbols Bond Graph Software).

The torques generated in the 3-axes for the H- drone are given by:

$$[(F3 + F2)(F1 + F4)]l1 = Tx \quad \text{Rolling (3)}$$

$$[(F1 + F2)(F3 + F4)]l2 = Ty \quad \text{Pitching (4)}$$

$$(M2 + M4 - M1 - M3) = Tz \quad \text{Yawing (5)}$$

Resultant thrust force in the z-direction is as follows:

$$F1 + F2 + F3 + F4 = Fz \quad (6)$$

Each propeller's Fi and Mi values (shown in Figure 1) are sent to the transformer, MTF, to compute the torques using equations (3)-(5). The resulting torques are then transmitted to the Euler Junction Structure (EJSR) to model the rotational dynamics at the drone's center of gravity (CG). EJSR can be represented as follows:

$$EJS_R = \begin{bmatrix} \dot{r} \\ \dot{p} \\ \dot{s} \end{bmatrix} X \begin{bmatrix} I_x \dot{r} \\ I_y \dot{p} \\ I_z \dot{s} \end{bmatrix} \quad (7)$$

With respect to the body frame, the angular velocities and moment of inertia of CG about the 3-axes (x,y and z) are given by r, p, s and I_x, I_y, I_z (I_i) respectively. Likewise, the calculation of the translational dynamics of the CG is done as:

$$EJS_T = \begin{bmatrix} x' \\ y' \\ z' \end{bmatrix} X \begin{bmatrix} mr \\ mp \\ ms \end{bmatrix} \quad (8)$$

Here, x', y', and z' denote the linear velocities of the CG around the x, y, and z axes, respectively, with respect to the body frame. The mass of the drone is represented by m. The linear and angular velocities obtained thus far are in the body frame; however, for trajectory control, they must be transformed into the inertial frame because the reference trajectories are in the inertial frame. Euler's angle transformation (roll ϕ, pitch θ, and yaw ψ) around the x, y, and z axes, respectively, which converts the linear velocities from the body frame to the inertial frame can be expressed as follows:

$$R_B^A = \begin{bmatrix} c\theta c\psi & s\phi c\theta c\psi - c\phi s\psi & c\phi s\theta c\psi - s\phi s\psi \\ c\theta s\psi & s\phi s\theta s\psi - c\phi c\psi & c\phi s\theta s\psi - s\phi c\psi \\ -s\theta & s\phi c\theta & c\phi c\theta \end{bmatrix} \quad (9)$$

In the inertial frame of reference, the external forces acting on the drone:

$$S_e = [0 \quad 0 \quad -mg]^T \quad (10)$$

Here, the term −mg represent the drone weight. Similar to the Newton-Euler method's equations, the bond graph derived dynamic equations are as follows [7].

$$m\begin{bmatrix} x \\ y \\ z \end{bmatrix} = \begin{bmatrix} 0 \\ 0 \\ F_z \end{bmatrix} + \begin{bmatrix} x \\ y \\ z \end{bmatrix} \times \begin{bmatrix} mr \\ mp \\ ms \end{bmatrix} + [{}_A R^B]^T \begin{bmatrix} 0 \\ 0 \\ -mg \end{bmatrix} \quad (11)$$

$$\begin{bmatrix} I_x \\ I_y \\ I_z \end{bmatrix} \begin{bmatrix} r \\ p \\ s \end{bmatrix} = \begin{bmatrix} T_x \\ T_y \\ T_z \end{bmatrix} + \begin{bmatrix} r \\ p \\ s \end{bmatrix} \times \begin{bmatrix} I_x r \\ I_y p \\ I_z s \end{bmatrix} \quad (12)$$

4. Selection Criteria

4.1 Frame Selection

The X-rotor frame was carefully selected to ensure a smooth fit for the 18 inch propellers, minimising any disturbance on the arms for maximum efficiency. Adequate space on the frame was also guaranteed for housing the necessary hardware and batteries. The structural integrity of the frame was examined through a static analysis on ANSYS, testing the arms for cantilever forces and moments to replicate the thrust from the motors. Further, CFD analysis was conducted on ANSYS Fluent to comprehend the aerodynamic interactions with the surroundings.

The selection of the X-rotor frame was based on important factors such as:

1. The lightest option
2. Having the longest motor arms
3. High torsional stiffness

The large frame was chosen for its suitability in open cast mining surveillance, as well as its ability to easily integrate crucial parts such as batteries, motors, propellers, GPS, and cameras. The design began with a 650 * 650 mm box with a variable height, and various subcomponents were subsequently designed and assembled with the help of 2D sketches provided by outsourced products.

NACA airfoils were extensively researched through CFD, ultimately leading to the selection of one Airfoil that met the specific requirements.

Table 3. Material of components.

Name of the components	Materials
X shaped links	Carbon fiber composite
Propellers (17 inches)	3D printed (nylon 6.6)
Various Mounts for cameras, sensors, batteries mount etc	3D printed (ABS)
Supporting base of the frame	Carbon fiber composite

4.2 Model

Figure 2. 3D Model of Quadcopter (Solid works).

4.3 ARM

The Arm of the drone would act as the bridge connecting the propellors to the chassis of the drone. We have designed the arm using topology optimization ensuring high strength to weight ratio. This also would be fabricated using nylon 6,6. The key feature of our arm is its ability to detach from the chassis during a malfunction.

It also makes it more modular and upgradable as the operator could easily switch arms based on the mission requirements this would help the drone to be ready faster for the missions.

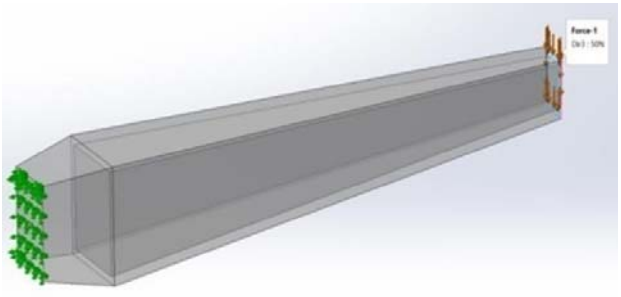

Fig 3. Force of 50N is applied to the face of the link, and fixed end conditions are also imposed during the process of topological optimization using solidworks

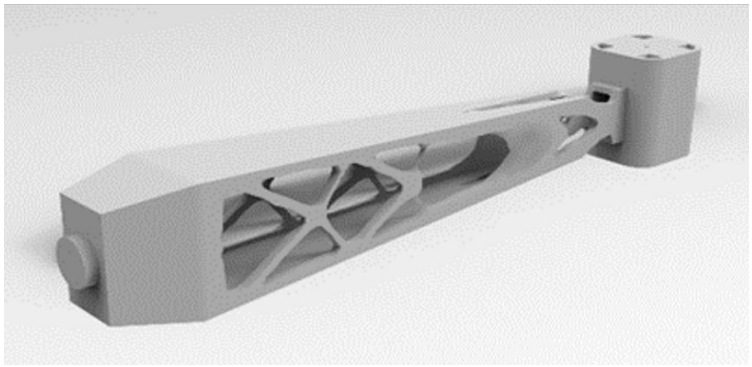

Fig 4. Rendered image of Link after topology optimization (Solid works)

4.4 Fixed-Pitch Propellers

These are the simplest and most commonly used propellers. They have a fixed angle of attack and are designed to provide a balance between efficiency and maneuverability. Fixed-pitch propellers are generally made of plastic or carbon fiber.

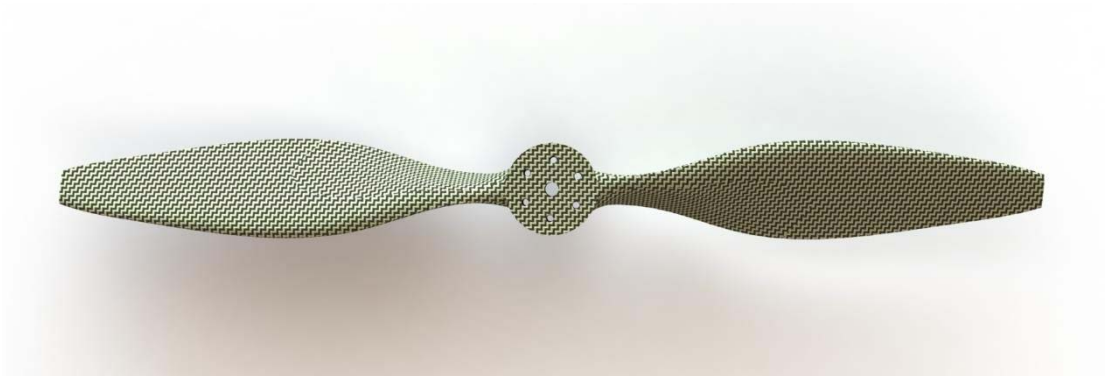

Fig 5. Rendered Image of Propeller (Solid works)

In the process of finishing the 3D CAD model obtained through reverse engineering, the NACA 4412 profile was utilized.

After analyzing the graph depicting the coefficient of lift (CL) versus the angle of attack (AOA), it was determined that the maximum angle of attack before stall should not exceed 15 degrees. Consequently, different angles of attack were selected in decreasing order (15,13.5,12,10.5 upto 0 degrees) for successive planes during the finishing process to ensure a smooth and optimal finish for the propeller. This approach takes into consideration the aerodynamic performance and stability of the propeller design.

4.5 Propulsion Selection

The selection of the propulsion system for the UAV was based on maximizing the thrust-to-weight ratio, fulfilling power needs, and accommodating the battery capabilities. By considering the initial weight predictions, the UAV was expected to weigh around 8 kg. To guarantee safety and proper maneuverability, a thrust-to-weight ratio near to 2:1 was ideal. The size of the airframe was 800 mm, which limited the size of the propeller to 458 mm. A thorough market research was carried out to find the best BLDC motor that met these constraints by using an online open-source software eCalc. The motor-propeller combination that showed suitable thrust characteristics were then evaluated based on their efficiency and

endurance. The required flight time was 20-30 minutes, and the motor-propeller configuration that provided this flight time with the least battery weight was selected. As per the initial calculations, the UAV needed a battery weight of 3.5 to 4 kgs for the necessary power and endurance. After evaluating the motor-propeller combinations, a 30,000 to 31,000 mAh, 45 to 60 C rated battery was needed. Considering all the above factors, the Sunny Sky (X4125-440) Motors and 18 x 6 inch propellers were chosen as the most efficient pair as it provides a flight time of 25 minutes with a 4130 gram, 5S-7P battery configuration. Finalized the thrust-weight ratio to 2.2 as higher the T/W ratio the easier it is to control the drone in elaborate aerobatics. The availability of motors and budget were also taken into account during the final decision-making process.

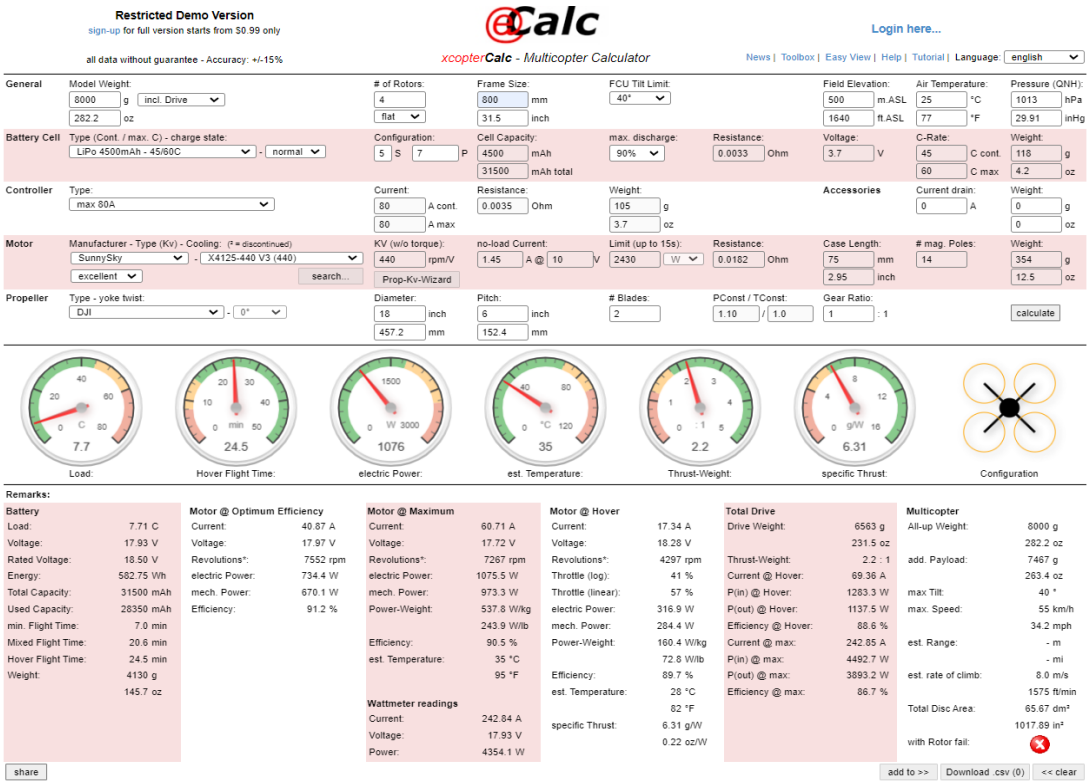

Figure 6. Propulsion Selection using eCalc software.

5. Surveillance and Mapping

Each mine has its own distinct set of obstacles that can be addressed by utilizing drones for tasks such as mine surveying, inventory control, estimating stock levels, and identifying problem areas. By using drones to survey mines, detailed information can be obtained about the site prior to beginning mining projects and any changes to the site over time can be tracked. Drones can also reach areas that are difficult to access and potentially hazardous, providing valuable insights for mine planning. In coal mines, drones can be used to locate potential areas of spontaneous combustion in coal stockpiles, allowing for preventative measures to be taken. Drones can also assist in managing the surrounding water sources, planning for blasts, optimizing haul routes, and responding to emergencies.

5.1 Steps Involved in Surveillance or Vision System

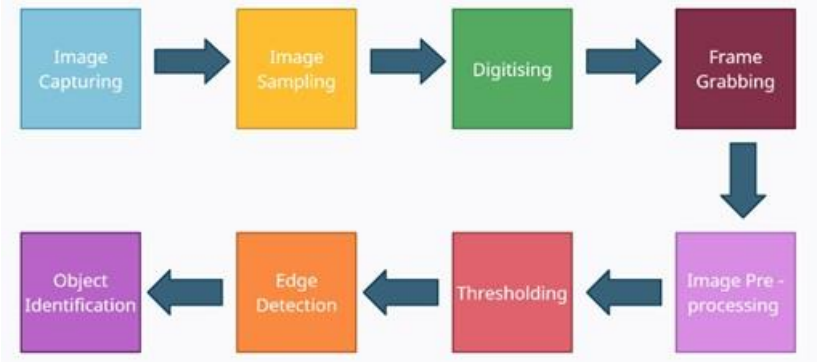

Figure 7. Flowchart of a Surveillance or Vision System.

5.1.1. Image Capturing. Image capturing involves acquiring an image from a vidicon or digital camera (CCD or CID), which is then stored in computer memory in formats such as TIFF, JPG, or Bitmap. While image acquisition is primarily a hardware function, software can be used to control various camera parameters. Image acquisition comprises a light source, a lens, an image sensor, and electronics to read the sensed image and transmit it to a computer for further processing.[8]

5.1.2. Image Sampling. A discrete grid of sampling points in the plane can be utilized to sample a continuous image f (x, y). The base Fourier transform is an example of an orthonormal function that can be used to expand the image function as a second option. The digitized image is then represented by the expansion's coefficients. In reconstruction algorithms, aliasing occurs when brightness values in nearby pixels are interpolated; this process is known as anti-aliasing and is frequently used in computer graphics. At sampling points, a continuous image is digitalized. The grid is the name given to the geometric relationship between these sampling points in the plane.[9]

5.1.3. Digitising. When processing images with a computer, an appropriate discrete data structure such as a matrix must be used to represent the image. Images captured by sensors are expressed as a continuous function f (x, y) in a two-dimensional plane. To digitize an image, the function f (x, y) is sampled into a matrix with M rows and columns. Image quantization assigns an integer value to each continuous sample, splitting the continuous range of the image function f (x, y) into K intervals. The higher the sampling rate (larger M and N) and quantization (larger K), the better the approximation of the continuous image function f (x, y) can be achieved. There are two important questions to consider when sampling an image function: first, determining the sampling period, which is the distance between neighboring sampling points in the image; and second, setting the geometric arrangement of the sampling grid.[9]

5.1.4. Frame Grabbing. The process of capturing a single frame from a video and converting it into a bitmap image involves the use of a frame grabber device. This device takes in the video source and captures the frame, converting it into a digital form. Modern frame grabbers have the capability to capture multiple frames simultaneously. Once captured, the resulting images can be manipulated to improve their quality or used for other applications.

5.1.5. Image Pre-Processing. Image pre-processing is a crucial step in image analysis that involves operations at the lowest level of abstraction. These operations aim to improve image quality by suppressing undesired distortions or enhancing relevant image features for further processing and analysis tasks. Although they do not increase image information content, they help to refine the image data.

Several different kinds of image pre-processing methods are available, such as pixel brightness transformations or brightness corrections, geometric transformations, image filtering and segmentation, Fourier transform, and image restoration. Each technique has its unique advantages and can be used for specific image processing tasks. [10][11]

5.1.6. Thresholding. Image thresholding is a fundamental technique that divides an image into a foreground and background. This is achieved by converting grayscale images into binary images using various thresholding algorithms. This technique is an important part of image segmentation, which is the process of dividing an image into multiple segments. Image thresholding is most effective in images with high contrast between foreground and background. Some common thresholding algorithms include histogram-based thresholding and multi-level thresholding. These algorithms can be applied to various types of images, including medical images and satellite images, to extract relevant information from them.[12]

5.1.7. Edge Detection. Edge detection is a fundamental method in image processing that finds edges or boundaries in digital image points with discontinuities, like sharp changes in image brightness. There are several methods for edge detection, including the Prewitt, Sobel, Laplacian, and Canny edge detection algorithms. Each of these algorithms has its advantages and disadvantages depending on the image being processed and the application for which the edge detection is being used.[13]

5.1.8 Object Identification The accuracy of identifying an object is determined by various attributes of the image. An AI system calculates a confidence score to predict the label or class of an object, but this process can be complex and requires a thorough understanding to achieve optimal results. Two important factors that influence the success of an object recognition algorithm are the efficiency of the algorithm and the number of objects or features present in the image. The goal is to align the image with the machine learning algorithm and extract relevant features to identify and locate the objects in it. These features may be either functional or geometrical in nature.[14]

5.2 Implementation

The goal of this project is to address challenges in the mining industry by utilizing a drone equipped with advanced hardware and custom software solutions.

5.2.1. Sensors. The drone will be equipped with EO/IR sensors, stereo cameras, and 2D/3D Lidars, which will provide a comprehensive and accurate view of the surrounding areas, allowing for more informed decisions in the mining process. The EO/IR sensor will provide high resolution live video feed to the mining operator when monitoring the mining field, and the operator will have the ability to select specific areas for a more detailed view, resulting in the drone reducing its altitude. Additionally, the drone will be equipped with thermal cameras for efficient surveillance during nighttime.[15]

5.2.2. Autopilot Selections. In this project, the UAV will be equipped with the ProfiCNC Pixhawk 2 (Hex Cube orange) autopilot system, which utilises the open-source firmware ArduPilot. The parameters of the ArduPilot can be adjusted to meet the specific needs of the mission and can be optimized for minimal mission duration and maximum accuracy and efficiency.
The Pixhawk Cube features built-in vibration-damping IMUs ICM 20602 and ICM 20948, an integrated magnetometer, and MS5611 barometer, and can connect to external sensors and computational units through various serial communication ports. The UAV also utilizes the Here3 GPS modules by ProfiCNC Hex, which offer high precision GNSS capabilities and support RTK navigation mode, are built with CAN protocol, dust and splash proof, equipped with STM32F302 processor, faster processing speed and better reliability, and have their own IMUs that can be used for improved position estimation. To control the actuators, the UAV is equipped with a servo rail that sends PWM signals to the ESCs, servos, and motor drivers in the system, providing exceptional localization and control.

5.2.3. Mission Planning. The goal of the project is to address challenges in mining by utilizing a drone equipped with a combination of hardware and custom-built software solutions. One aspect of this includes creating a path for the drone that allows it to cover the entire mining area while using the least amount of flight time. To achieve this, a ground control software is necessary that is able to plan, save, and load autonomous missions into the drone's autopilot[16]. This software, known as a ground station, communicates with the drone through wireless telemetry and can display real-time data on the drone's performance and position. Additionally, it can be used to control the drone in flight, upload new mission commands and set parameters, and monitor live video streams from the drone's cameras. After researching various options, the team decided to use the Mission Planner software, which is compatible with Windows and can be used for different types of autonomous vehicles like Copter, Plane, Rover and Antenna Tracker. The UAV autopilot is installed with Ardupilot firmware and waypoint[17] following scripts were tested in simulation.

Figure 8. Path planning done by adding waypoints in the simulator (Ardupilot firmware).

5.3 Mapping

In open cast mining, mapping the terrain and the structure of the mine can help in making better technical decisions by understanding the data and knowledge of the terrain. This is done using Computer Vision, where multiple images with narrow but overlapping fields of view are combined to create a larger image with a wider field of view. In this project, input from an RGB camera is used in a mapping algorithm that detects key points and retrieves local invariant descriptors using the Scale-Invariant Features Transform (SIFT) and Speeded Up Robust Features (SURF) algorithms. If the number of common invariant descriptors exceeds a threshold value, they are matched between the two input image frames and a Homographic matrix is determined to help create a single stitched map out of the two images. This process is repeated with new input frames, and the algorithm is optimized to be insensitive to image ordering, orientation, illumination and noise parameters. Robust gain compensation and image blending algorithms are also used to improve the appearance of the final stitched map.

5.4 Mapping Implementation

The algorithms mentioned above were tested on a UAV in a complex. An area of 100*100 m2 was covered by the UAV. The images obtained were stitched together to obtain the final image. The algorithm was tested twice in two different flights and the resultant stitched image[18] is presented below:

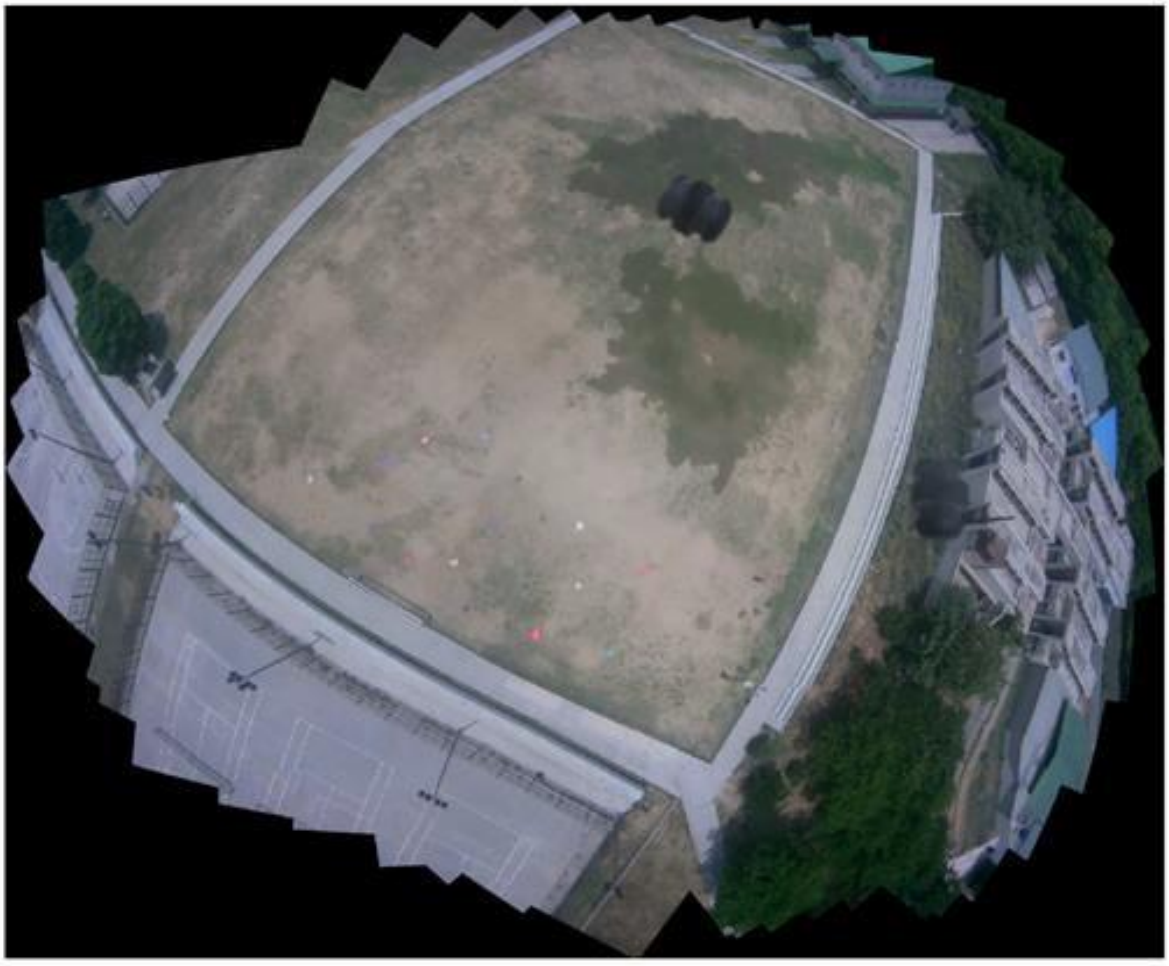

Figure 9. Stitched Image Obtained using N numbers of image captured in a sequence using EO/IR sensors, stereo cameras, and 2D/3D Lidars.

6. **Stockpile Volume Estimation and Slope Stability**

6.1. Introduction

High-tech sensors installed in Unmanned Aerial Vehicles (UAVs) provide many benefits, particularly for quickly collecting data within a specific time frame. This study aimed to examine the accuracy of measuring stockpile volumes using UAVs. The objectives of the research were to assess errors in field measurements and high-precision volume calculations, to map the volume of stockpiles[19] using UAV images, and to calculate the time needed for the survey. The imaging process was performed using a UAV, while the detailed survey was carried out through Laser Scanning to compare and verify the accuracy of both methods. The stability of slopes in open-pit mines is a significant concern due to the potential detrimental effects of instabilities. To ensure the safe and efficient operation of these mines, it is necessary to evaluate and manage slope stability risks systematically. However, this has traditionally been challenging as measuring the necessary parameters for assessing slope stability can be labor-intensive, costly, and disruptive to mining operations. Therefore, for risk assessment of slope stability, we propose using a UAV equipped with Lidar sensors to detect fractures and crevices in stockpiles. By analyzing this data, a risk assessment can be created that could help predict various accidents and hazards in the mine.

6.2. Stockpile Estimation-Mapping Techniques

There are various types of mapping techniques for estimating stockpiles, such as:

6.2.1 3D point cloud: We can create a 3D point cloud from drone data that contains geospatial (X, Y, Z) and color information for each point. When compared to 3D mesh models, 3D point clouds offer precise data without the distortion [20]. This approach, which is regarded as the industry standard, provides incredibly detailed models for calculating distance (both vertically and horizontally), area, and volume.

Figure 10. Stockpile Estimation using 3D Point Cloud (open-source image).

6.2.2 Orthomosaic maps: A large, map-like image known as an orthomosaic is produced by geometrically correcting aerial photographs. Lens distortion, camera tilt, perspective, and topographic relief are some of these corrections. Each pixel on the image contains 2D and 3D geospatial data (X, Y), allowing for quick and accurate measurements. We can precisely measure the area, volume, and distance of projects thanks to orthomosaic maps.

Figure 11. Stockpile Estimation using Orthomosiac Maps (open-source image).

6.2.3 3D textured mesh: A triangle-based surface known as a 3D textured mesh can be created using the point cloud. This model minimises the distances between the points on the point cloud and thesurface while accurately reflecting the edges, faces, vertices, and texture of the area that the drone captured. This model is appropriate for projects requiring public participation or visual inspections.

Figure 12. Stockpile Estimation using 3D Textured Mesh (open-source image).

6.2.4 Digital terrain model (DTM): Digital Terrain Models (DTMs) are frequently made from drone images, with each pixel containing 2.5D data (X, Y, and Z value of the highest elevation). Each collected image must have enough overlap for a DTM to be created accurately. Calculations using digital terrain models are quick and accurate.

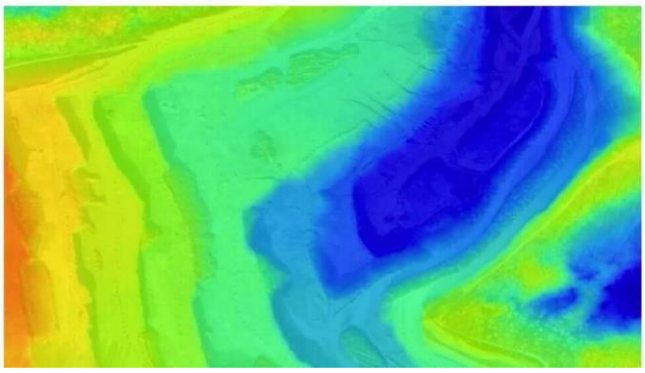

Figure 13. Stockpile Estimation using Digital Terrain Model (generated using python (GeoSlam software)).

7. **Volume Estimation Methods**

7.1 Method 1

A machine learning model is trained to estimate the volume of stockpiles using 2D images from a top-down camera on a UAV. This method typically involves performing a 3D reconstruction of the area through the use of dense matching and multiple views, as well as exploring methods such as site-specific heuristics or shape from shading. Once the 3D geometry is calculated, various techniques can be used to measure the volume, including cross-section and horizontal section methods. The scene is frequently divided into small elementary 3D volumes like voxels, tetrahedrons, or trigonal prisms or into Digital Surface Models (DSMs), which are 2D grids with an altitude value assigned to each cell for more precise estimates on irregular shapes. In most cases, segmentation and subtraction of a bare terrain model are combined to determine the boundaries of the piles.

7.2 Method 2

A 2.5D map is created using parallax mapping and multiple images to estimate depth.
The volume is then calculated using Cloud Compare and the stockpile is isolated. Using surface reconstruction algorithms, we can turn the point cloud into a mesh. However, by taking advantage of a stockpile's special property—that the surface is constrained by the XY plane and no two points have the same x and y—this method can be avoided. By projecting the PCD to the XY plane and removing the Z value, we can use the Delaunay algorithm to triangulate the surface reconstruction in 2D space. Then, instead of using the 2D vertices that Delaunay produced, we will use the 3D vertices. "Delaunay 2.5D" is another name for this strategy.

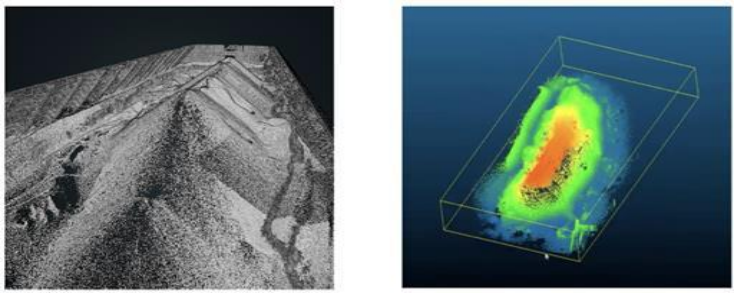

Figure 14. 2.5D map is created using parallax mapping and multiple images to estimate depth.

7.3 Volume Estimation Using Lidar

The process of volume estimation involves a few key steps, including manual isolation of stockpiles[21], manual estimation using Civil 3D or Cloud Compare, and the use of the Open3D Python Library for PCL analysis. The Open3D[22] library offers various functions such as down sampling PCLs, creating triangular meshes, plane segmentation, and bounding volumes. These functions are being tested in conjunction with deep learning techniques in order to automate the process of stockpile volume estimation. Researchers are using publicly available stockpile point clouds and attempting to remove unwanted points, segregate the stockpile from noise, and build a triangular mesh. The volume below each triangle is then calculated and added together to estimate the total volume of the stockpile. The left image shows the raw PCL after removing the ground points, while the right image depicts the mesh overlaid on top of the PCL.

7.4 Volume Estimation Using Deep Learning

The use of deep generative architectures, such as the 3D Adversarial Autoencoder (3dAAE), allows for the modelling of intricate 3-dimensional objects, like point clouds. This specific architecture can be used to gain significant representations of 3D shapes which can be employed for difficult tasks including generation, reconstruction, compression, and clustering of 3D points. The 3D Adversarial Autoencoder (3dAAE) takes 3D input and produces 3D output in the form of point clouds. It can be used to obtain either a binary or continuous latent space that encompasses a broad range of the training data distribution. This type of autoencoder can simplify the complexity of stockpile data that is in the form of point clouds while maintaining its geometric characteristics.

8. **Vulnerability Assessment of Slopes in Open Cast Mines**

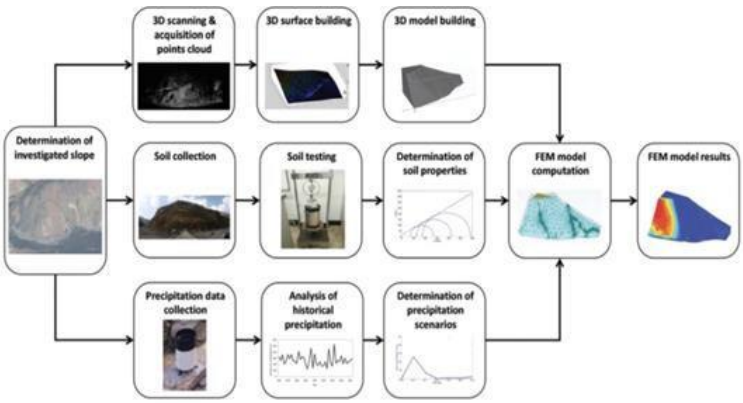

Figure 15. Methodology for slope stability analysis using laser scanning and numerical simulation.

- 3D scanning and data acquisition
- Reconstruction of slope geometry
- 3D FEM model
- FEM Analysis

8.1. Steps for assessment:

1) The proposed approach has been evaluated and found to be effective in obtaining detailed 3D geometry information of slopes and generating computable FE models for analysis. This method can be used to assess the safety of slopes and identify potential failure surfaces, providing valuable insights into the physical processes of slope failure and tools for examining the safety of specific sites.

2) The precision of the modelled slope geometry is crucial for accurate slope stability analysis results. It is important to find a balance between detailed geometry and computation cost.

3) The results of the case study indicate that the slope is approaching a failure state. It is recommended to implement engineering measures to monitor and mitigate the stability limitations of the slope to reduce the risk of disasters.

9. **Conclusion**

In conclusion, the following literature presents the development of an unmanned aerial vehicle (UAV) for real life applications such as coal mines surveillance, hazard detection and other similar uses. For the first stage of the study, a multi-rotor quad-copter is designed considering various parameters such as VTOL, Maneuverability, Hover efficiency etc. In the next part, Dynamic Modelling of the quadcopter is undertaken using the Bond Graph Method. The 3D model designed in Solid works has been imported into Ansys and static structural analysis has been performed. The induced total deformation in the entire frame of the quadcopter has been calculated. The propulsion system selection has been based upon maximizing the thrust-to-weight ratio to 2.2:1, ensuring optimal factor of safety of about 4 and maximizing maneuverability. An online open-source software namely eCalc has been utilized for calculating the most apt motor-propeller combination for ideal thrust characteristics. In the last few sections of the literature, the steps involved in surveillance and the mapping techniques have been discussed. An 8-step methodology is presented for the image identification. After the image capturing, mapping implementation has been performed using stitching of N sets of images (with the help of optimal path planning using waypoints added throughout the targeted area in a sequence) to obtain the final image. Also, the stockpile volume estimation methods and mapping techniques are presented (literature research) which may lead to final the estimated depth of the coal field or slope of the terrain with the help image data which we captured with the help of 2.5D cameras, lidar sensors, proper path planning etc. In the final section of the literature, steps are presented for the vulnerability assessment of slopes in open cast mines.

References

[1] Ren H, Zhao Y and Xiao W 2019 A review of UAV monitoring in mining areas: current status and future perspectives *Int J Coal Sci Technol* ***6***, pp. 320–333
[2] Ebrahim M 2016 3D laser scanners: history, applications and future *LAP LAMBERT Academic Publishing* **104**
[3] Heidemann H K 2018 Lidar base specification (ver. 1.3, February 2018): *U.S. Geological Survey Techniques and Methods*, book 11, chap. B4. (October 2014), 101
[4] Bawden W F 2015 The expanding impact of technology on underground geomechanically mine design and operations — advances, limitations and future needs. *Underground Design Methods*
[5] Bhandari G, Pathak P M and Saha S K 2022 Bond graph modeling and trajectory control of H- drone *13th Asian Control Conference (ASCC),* Jeju, Korea, Republic of, 2022, pp. 2206-2211
[6] Siciliano B and Khatib O 2016 Robotics and the handbook *Springer Handbook of Robotics*, pp. 1-6. Springer, Cham
[7] Luukkonen T 2011 Modelling and control of quadcopter *Independent research project in applied mathematics*, Espoo, 22, p.22
[8] Saha S K 2008 *Introduction to robotics* McGraw-Hill Education (India)
[9] Azad M M, Hasan M M, and Alam A 2011 Digitizing and sampling of image process
International Journal of Research and Reviews in Computer Engineering Vol. 1, No. 1
[10] Haralick, Robert M, and Linda G S 1992 Computer and robot vision *Addison-Wesley*, Vol. I
[11] Sonka M, Hlavac V and Boyle R 1998 Image processing, analysis and machine vision *PWS Publishing*
[12] Kang B-H 2007 A review on image and video processing *International Journal of Multimedia and Ubiquitous Engineering* **2**, 2
[13] Ansari Mohd A, Kurchaniya D, and Dixit M 2017 A comprehensive analysis of image edge detection techniques *International Journal of Multimedia and Ubiquitous Engineering*, **12**(11), pp. 1–12
[14] Object Detection and Tracking 2013 *Object Detection and Recognition in Digital Images*, 346– 407
[15] Park S and Choi Y 2020 Applications of unmanned aerial vehicles in mining from exploration to reclamation *A Review:Minerals* **10,** 663
[16] https://ardupilot.org/planner/docs/mission-planner-overview.html
[17] https://ardupilot.org/planner/docs/common-planning-a-mission-with-waypoints-and-events.html
[18] Bhadane D and Pawar K N 2016 A review paper on various approaches for image mosaicing
International Journal of Engineering and Management Research (IJEMR)
[19] Reynaldo M. Gago, Matheus Y. A. Pereira, Guilherme A. S. Pereira An aerial robotic system for inventory of stockpile warehouses , *Wiley Online Library Engineering Reports*
[20] Scans Forte, M., Neto, P., Thé, G. and Nogueira, F. Altitude Correction of an UAV Assisted by Point Cloud Registration of LiDAR *18th International Conference on Informatics in Control, Automation and Robotics (ICINCO 2021), SCITEPRESS – Science and Technology Publications*
[21] https://samples.geoslam.com/Potree/stockpile/stockpile.html
[22] https://jose-llorens-ripolles.medium.com/stockpile-volume-with-open3d-fa9d32099b6f